soil systems

MDPI

Article

Soil De-Sealing and Recycled Aggregates Application: One Year of Monitoring

Gaia Mascetti *, Roberto Comolli, Francesca Pittino, Isabella Gandolfi and Chiara Ferré

Department of Earth and Environmental Sciences, University of Milano-Bicocca, Piazza della Scienza 1, 20126 Milan, Italy; roberto.comolli@unimib.it (R.C.); francesca.pittino@unimib.it (F.P.); isabella.gandolfi@unimib.it (I.G.); chiara.ferre@unimib.it (C.F.)

* Correspondence: g.mascetti2@campus.unimib.it

Abstract

De-sealing, or depaving, is increasingly adopted to restore soil permeability and support green infrastructure, yet its potential to recover soil functions remains insufficiently understood. This study reports one year of soil monitoring following the de-sealing of a brownfield site in Milan (Italy). It compares the evolution of pedoclimatic parameters in sealed and de-sealed soils and assesses the suitability of recycled aggregates (RAs) from demolition waste as a soil-forming material. Buried sensors continuously recorded pedoclimatic parameters, temperature, water content, and oxygen concentration, while periodic sampling was carried out to analyse soil chemical properties, bacterial community composition, and the quality of percolation water (heavy metal content). De-sealing immediately improved pedoclimatic conditions, enhancing soil aeration, water regulation, and heat exchange capacity. No significant variation was detected in soil chemical properties, apart from pH fluctuations linked to the leaching of alkaline ions from concrete-based RAs. The presence of RAs caused no adverse effects on either soil or percolation water. Bacterial community composition was strongly associated with soil organic carbon, C:N ratio, and soil water content, without showing clear temporal trends. Overall, the study demonstrates that de-sealing rapidly triggers soil functional recovery and that, when properly characterised for composition and contamination risk, RAs pose no evident threat to the surrounding environment.

Keywords: soil sealing; de-paving; soil recovery; construction and demolition waste (C&DW); recycled aggregates (RAs); soil properties; soil microclimate; pedoclimatic parameters; soil bacterial communities

Academic Editor: Remigio Paradelo Núñez

Received: 23 September 2025
Revised: 7 November 2025
Accepted: 10 November 2025
Published: 14 November 2025

Citation: Mascetti, G.; Comolli, R.; Pittino, F.; Gandolfi, I.; Ferré, C. Soil De-Sealing and Recycled Aggregates Application: One Year of Monitoring. *Soil Syst.* **2025**, *9*, 128. https://doi.org/10.3390/soilsystems9040128

1. Introduction

Soil sealing is the permanent covering of soil with impermeable artificial materials such as asphalt, concrete, or paving stones. Driven by urbanisation, it causes rapid land consumption, often at the expense of arable land [1], and is a major driver of soil degradation in Europe [2,3]. It disrupts interactions among the soil, atmosphere, and hydrosphere, disturbing biogeochemical and hydrological cycles and impairing soil functions and ecosystem services. The most evident consequences include habitat loss and fragmentation, reduced soil productivity and infiltration capacity, and an intensification of the urban heat island effect [3].

In recent decades, de-sealing (or depaving) has emerged as an important strategy to mitigate and offset the impacts of soil sealing and to support European targets for reducing

land take and achieving the Sustainable Development Goal of making cities and human settlements inclusive, safe, resilient, and sustainable [4]. The process entails removing the impermeable surface layer, followed by the decompaction of underlying materials and their replacement with a permeable pavement or the reconstruction of the soil profile [5–7].

Numerous de-sealing projects have already been implemented worldwide, ranging from large-scale urban regeneration initiatives, such as converting railways, airports, or brownfields into mixed-use developments [8], to small-scale actions led by communities, associations, and local stakeholders [9]. These smaller efforts often target over-paved public areas (e.g., squares, car parks, and residual urban spaces), fostering the creation of green areas, parks, and community gardens. Integrating such interventions into a coherent, well-planned green infrastructure network is essential to maximise ecological benefits and can significantly enhance urban biodiversity [7,8]. In Italy, several cities have recently adopted depaving strategies; however, according to ISTAT data, the increase in per capita urban green space has been modest, rising from 31.9 m^2 in 2011 to 33.3 m^2 in 2023 [10], suggesting that current efforts remain insufficient to offset ongoing soil sealing and that broader de-sealing interventions are urgently needed.

De-sealing is currently applied primarily to restore soil permeability and implement green infrastructure [11], thereby enhancing urban resilience to flooding and heatwaves [9]. A survey of French cities [7] confirmed that the main goals of de-sealing interventions are sustainable rainwater management and heat mitigation. De-sealing also plays a key role in restoring biodiversity across multiple ecological levels by creating favourable conditions for the establishment of plants, animals (such as nematodes, arthropods, and earthworms), prokaryotes, and fungi. Among these groups, all essential for improving soil properties and functions [12], prokaryotic communities are the main biological drivers of biogeochemical cycles. They are involved in the decomposition of organic matter, including organic carbon mineralisation, nitrification, denitrification, and phosphorus solubilisation. By converting chemical compounds into nutrients available to other organisms, these microorganisms enhance soil fertility and functionality [13].

Despite its advantages, de-sealing must be implemented with technical rigour, involving site-specific assessments to identify existing contamination, detect possible pollutant migration pathways, and evaluate the feasibility of the intervention. Information on soil and material properties is also crucial to ensure the effectiveness and long-term sustainability of de-sealing projects [7,14], depending on the intended post-intervention use. However, there are still no specific guidelines or tools for optimising de-sealing and soil restoration practices [7].

According to Caselli et al. [9], de-sealing has appeared in the scientific literature since the 1990s. Yet research has mainly focused on its integration into urban planning, with limited attention to its direct role in soil restoration and multifunctionality. Its significance as an independent soil management strategy has only recently been recognised [9]. Recent studies have demonstrated the benefits of de-sealing for urban and peri-urban environments [15] and have shown that unsealed soils can regain their functions and, consequently, provide associated ecosystem services even without direct intervention, particularly when colonised by spontaneous vegetation [12]. Nevertheless, the recovery of physical, chemical, and biological fertility in newly de-sealed soils can be enhanced through decompaction and targeted treatments [6]. These typically involve applying exogenous topsoil, sometimes enriched with organic or mineral amendments, to improve soil properties and facilitate plant establishment [3,6,7]. De-sealed soils are often subsequently vegetated by seeding or planting appropriate species selected according to soil characteristics, climate, and intended land use [7,11]. A well-adapted plant cover can improve soil quality, support biodiversity, strengthen urban resilience to climate change, and reduce maintenance requirements [7].

However, the extraction, transport, and application of imported topsoil entail significant economic and environmental costs, including the loss of agricultural land and increased CO_2 emissions [3,7]. In line with circular economy principles, a more sustainable alternative is to reuse locally derived materials, following a detailed assessment of their composition, quality, and contamination risk [7]. According to Villeiard et al. [7], recent studies have explored the reuse of various organic and mineral waste materials, including construction and demolition waste (C&DW). The inert, non-hazardous fraction of C&DW (CER 17 09 04) [16] can be processed into recycled aggregates (RAs) through on-site crushing and screening [17] and reused according to their properties and composition. For instance, concrete waste from underground structures can yield high-quality RAs suitable for structural applications, while mixed C&DW can produce aggregates for non-structural uses such as backfilling [16]. The on-site reuse of RAs exemplifies applied circular economy principles, reducing both the economic and environmental costs associated with transporting and disposing of C&DW, the largest waste stream in Europe, accounting for approximately 40% of total waste [18]. In recent years, several de-sealing projects, such as those in Dunkerque and Auberville (France), have reused asphalt blocks and demolition debris in situ as substrate material for urban green installations [8]. Scientific trials have indicated that RAs can serve as cost-effective and promising soil-forming materials [1,19]. However, the environmental safety of recycled aggregates strongly depends on their composition, particle size, degradation rate, and potential contamination risks, including alkalinity or heavy metal release. Moreover, since RAs are largely inorganic material, their use in soil reconstruction may require the addition of organic amendments.

Overall, de-sealing represents a valuable and increasingly adopted strategy for mitigating the impacts of soil sealing and supporting urban regeneration. However, as a relatively new topic in soil science, its potential to restore soil multifunctionality—physical, chemical, and biological functions supporting soil health—remains poorly understood. Previous studies have primarily investigated individual soil functions, such as enhanced permeability [15], and selected aspects of chemical and biological fertility [6,12]. To date, some research has examined the effects of de-sealing and revegetation on the urban microclimate [20], but no studies have assessed pedoclimatic parameters in sealed and de-sealed soils or their relationships with soil biological and physical processes. Moreover, despite growing interest, few studies have evaluated the effects of recycled aggregates on soil properties and functions [1,19], and none under real field conditions. Given the high heterogeneity of RAs, arising from the variable composition and origin of their parent C&DW materials, further research is essential to assess their performance and suitability as soil reconstruction materials.

This study addresses these gaps through a field monitoring experiment that integrates pedoclimatic and microbiological analyses in de-sealed urban soils amended with RAs. Specifically, it presents the results of one year of monitoring following a de-sealing intervention aimed at promoting soil functional recovery and assessing the use of recycled aggregates as a soil-forming material and growth substrate for vegetation. The study objectives were to: (i) compare the evolution of pedoclimatic parameters (temperature, water content, and oxygen concentration) in sealed and de-sealed soils; (ii) monitor changes in soil properties and bacterial communities in de-sealed soils; and (iii) evaluate these outcomes in relation to the addition of RAs as a soil-forming material.

2. Materials and Methods

2.1. Study Area and Experimental Design

The study area lies within a broader de-sealing experimental site, an urban brownfield in south-eastern Milan, Italy (45°25′27.0″ N; 9°14′0.9″ E), managed by the Urban Forestry Centre (CFU), the operational branch of the national association "Italia Nostra". In 2022, a preliminary soil investigation was carried out on the soils of the study area which, being sealed, were classified as Ekranic Technosols [21]. The investigation confirmed the absence of soil contamination beneath the sealing layer and the feasibility of the de-sealing project.

De-sealing was carried out in October 2023, following project approval, acquisition of equipment, and coordination with the CFU. After removal of the concrete cover, a pedological survey was conducted by opening and describing four soil profiles (Figure S1; Table S1). The profiles revealed weakly developed, base-saturated soils with surface layers formed from material moved by intentional human activity, classified as Eutric Transportic Regosols [21]. The bacterial communities in these profiles were analysed using the same methods described in Section 2.4 (Figure S2).

The de-sealing and soil characterisation were completed on 17 October 2023 (time zero, t_0), marking the start of discrete monitoring of soil properties. The following week, a soil monitoring system comprising 16 buried sensors was installed to continuously record soil temperature (T), soil water content (SWC), and soil air oxygen concentration (O_2) from 26 October 2023 to 29 October 2024.

Sensors were placed approximately 30 cm below both the newly exposed soil surface in four experimental plots (D1–D4) and beneath the remaining concrete pavement at two sites (S1 and S2; Figure 1a), to monitor pedoclimatic conditions under three scenarios: de-sealed soil, centrally sealed soil (S1), and sealed soil at the pavement edge (S2). The latter represented a partially sealed condition caused by edge effects, typical of road and sidewalk margins. Owing to the malfunction of the oxygen sensor at the central sealed position (S1), a theoretical oxygen concentration of 1% v/v was assumed for well-sealed soil, representing anaerobic conditions in line with literature values for oxygen depletion under impermeable layers [22–24].

In the unsealed plots, additional temperature and soil water content sensors were installed at a 10 cm depth (Figure 1b) to assess vertical gradients in temperature and moisture. All sensors (SO-110 oxygen sensors, Apogee Instruments Inc., Logan, UT, USA; Teros-11 soil water content and temperature sensors, METER Group AG, Munich, Germany) were connected to a data acquisition system comprising a Campbell Scientific AM16/32B multiplexer and CR300 data logger (Campbell Scientific Inc., Logan, UT, USA), powered by a 12 V–60 Ah gel buffer battery. The system was programmed for hourly data collection and housed in a waterproof container. On-site meteorological parameters (air temperature and precipitation) were also recorded using a Rain Gauge RG3-M equipped with a HOBO Data Logger UA-003 (Onset Computer Corporation, Bourne, MA, USA), to provide contextual environmental data.

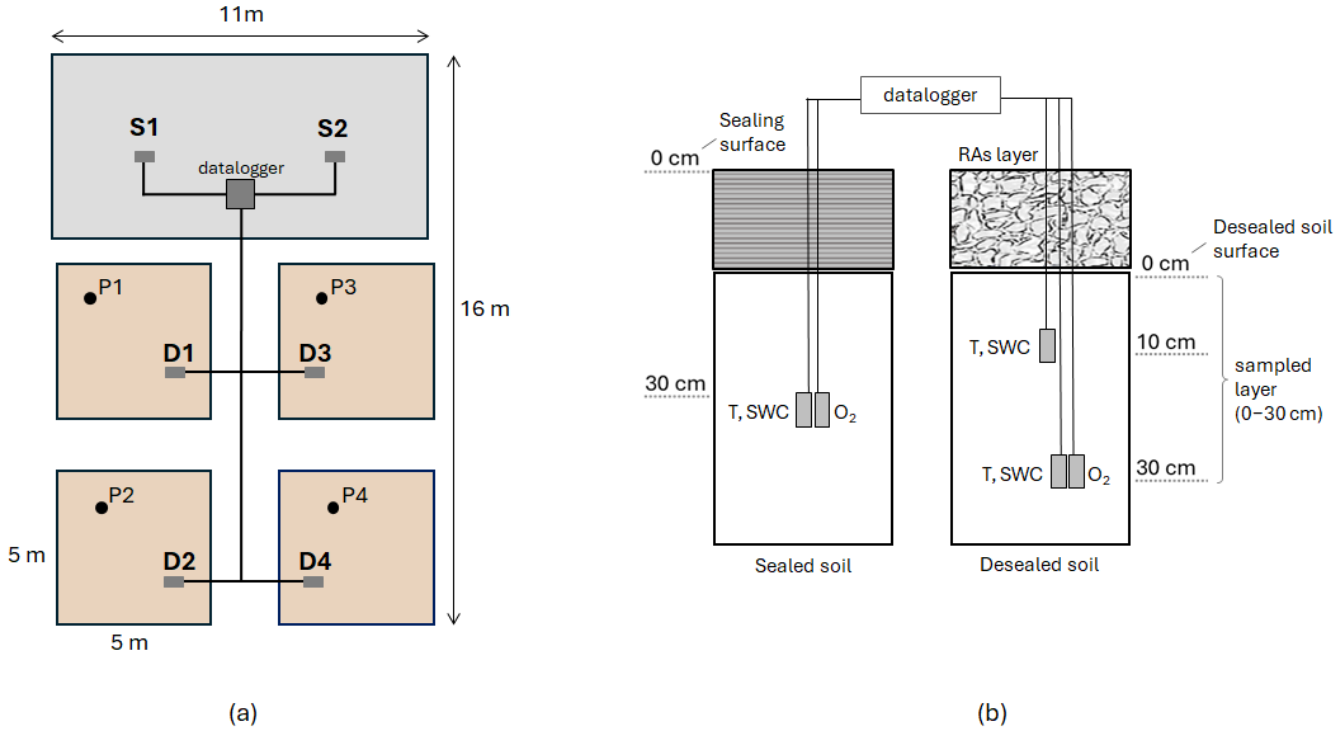

Figure 1. Experimental design and soil monitoring system. (**a**) Spatial distribution of sensors in de-sealed (D1, D2, D3 and D4) and sealed soil (S1 and S2). The figure also shows the location of the soil profiles (P1, P2, P3 and P4) in the experimental plots. (**b**) Graphical representation of the sensors buried under the pavement and RA layer in sealed and unsealed soil respectively, for the monitoring of temperature (T), soil water content (SWC) and oxygen (O_2) in soil air.

Specially designed drainage lysimeters, i.e., cylindrical soil-filled containers open at the top to allow water infiltration and equipped with a collection system at the base, were also installed in the unsealed soil to collect percolated water and detect any contaminants potentially released by the use of RAs. The recycled aggregates, obtained from crushed concrete pavement, were evenly spread over the de-sealed soil to form a 20 cm layer serving as a soil-like substrate for vegetation growth. Five lysimeters were installed: four within the experimental plots (one per plot) and one in a control area adjacent to the site, where the unsealed soil was left uncovered by the RA layer.

According to national and European regulations [25], demolition waste from the concrete pavements and, in part, from abandoned buildings was characterised and classified as non-hazardous (CER 17 09 04) [16]. This material was then crushed and sieved to a maximum particle size of 4 cm to produce RAs, composed mainly of concrete, sand, bricks, and stones, with traces of metal, glass, rubber, and plastic. Before field application, the producer carried out a leaching test on the RAs.

On 5 April 2024, green waste compost was incorporated into two plots (D3 and D4), and all plots were subsequently sown: two with a monoculture of *Sorghum bicolor* (D1 and D3) and two with a mixture of *Lolium* and *Trifolium* species (D2 and D4).

2.2. Soil Sampling and Analyses

Changes in the properties of the unsealed soil were monitored through periodic sampling of the 30 cm soil layer immediately beneath the 20 cm RA layer (Figure 1b). From October 2023 to January 2024, soil samples were collected monthly using a composite sampling approach. After removing the RAs with a shovel, three samples were taken from each plot using a gouge auger and then combined. Subsequently, sampling was performed every three months, in April, July, and October 2024, for a total of seven sampling events.

These later samples were not collected using the composite method, as it can damage vegetation. Instead, each plot was divided into two halves: one for monitoring vegetation growth and the other subdivided into three smaller subplots (approximately 1.5 m × 2 m each). One soil sample was collected from each subplot at every sampling time.

Samples were air-dried at room temperature and sieved (2 mm mesh) for standard laboratory analyses: pH (measured potentiometrically in a 1:2.5 soil-to-water ratio), total carbonates (Dietrich-Frühling method), soil organic carbon (SOC), and total nitrogen (Flash EA 1112 NC-Soil elemental analyser, Thermo Fisher Scientific CN, Pittsburgh, PA, USA).

2.3. Leaching Test and Percolation Water

The potential release of pollutants from the RAs was evaluated before their application in the field. The leaching test, conducted by the RA supplier and detailed in the Supplementary Materials (Table S2), showed that the RA eluate had a slightly alkaline pH (8.7) and low concentrations of major ions (nitrates 34.6 mg/L, sulphates 244 mg/L, chlorides 6.3 mg/L), all below the regulatory limits. Likewise, concentrations of potentially toxic metals, including Cu (0.006 mg/L), Zn (<0.001 mg/L), Ni (2.61 µg/L), Pb (<10 µg/L), and Cd (<1 µg/L), were well below reference thresholds. These results confirmed that the RAs were safe for use in soil reconstruction under the conditions of this study.

Percolation water was subsequently collected from the lysimeters every one to two months, depending on rainfall frequency and intensity, using a vacuum pumping system. The total concentrations of heavy metals (Pb, Cu, Ni, Cr, Zn) were determined by atomic absorption spectroscopy (AAnalyst 200 Atomic Absorption Spectrometer, PerkinElmer Inc., Waltham, MA, USA). Finally, metal concentrations were normalised to the volume of percolation water collected from each lysimeter.

2.4. Bacterial Community Characterisation

Soil sampling for the analysis of the bacterial communities was carried out as described above for the soil properties, using nitrile gloves and cleaning all the equipment with ethanol prior to collecting each sample. Within 24 h, approximately 5 g of each sample were stored at −20 °C until further processing. For the characterisation of the bacterial community, total DNA was extracted from 0.5 g of each soil sample using the FastDNA™ Spin Kit for Soil (MP Biomedicals, Solon, OH, USA), according to manufacturer's instructions. Then, the V5–V6 hypervariable regions of the 16S rRNA gene were amplified by PCR using 783F and 1046R primers, and the resulting amplicons were sequenced by MiSeq Illumina with a 2 × 300 bp paired end protocol (Illumina, Inc., San Diego, CA, USA), as described in Nava et al. [26]. Sequence processing and Amplicon Sequence Variants (ASVs) inferring and classification were carried out as described in Gandolfi et al. [27].

2.5. Data Processing and Analysis

All statistical analyses and data processing were performed using RStudio software, version 4.4.2. After processing the raw sensor data as described in Appendix A, a comprehensive pedoclimatic dataset was compiled by integrating daily data from 26 October 2023 to 29 October 2024. Missing values were estimated by linear interpolation, accounting for air temperature variations to ensure full temporal coverage (n = 370 observations). Summary statistics (mean, standard deviation, minimum, and maximum) were calculated for each variable and grouped by meteorological season, soil cover condition, experimental treatment, and soil depth to enable comparative analyses. Seasonal variations were assessed according to meteorological seasons (Winter: December–February; Spring: March–May; Summer: June–August; Autumn: September–November).

The effects of de-sealing, compost addition (CoA), and vegetation type (VgT) were analysed using mean values: D1–D2–D3–D4 (de-sealed plots), D3–D4 (with compost),

D1–D2 (without compost), D1–D3 (*Sorghum*), and D2–D4 (mixed grass). The effects of CoA and VgT on unsealed soil parameters were evaluated over the period from 5 April 2024 to 29 October 2024 (n = 203 observations). As all environmental variables remained non-normally distributed after transformation (Shapiro–Wilk $p < 0.001$), Cliff's delta was applied to obtain robust, non-parametric estimates of effect size. Cliff's delta represents the probability that a random observation from one group exceeds that from another. To account for temporal dependencies, 95% confidence intervals were computed through bootstrap resampling (1000 iterations), preserving the temporal structure of the data while providing reliable uncertainty estimates.

Temporal changes in soil properties were analysed using linear mixed models, with experimental plot included as a random factor (lme function). Spatial independence of residuals was assessed using Moran's I test based on a nearest-neighbour weight matrix. Model validity was checked with the Shapiro–Wilk test, and model selection was based on the Akaike Information Criterion (AIC). Accordingly, pH, $CaCO_3$, and C:N ratio were transformed using logarithmic, Yeo–Johnson, and Box–Cox transformations, respectively. Significant temporal differences between sampling dates (categorical variable) were evaluated through post hoc Tukey's tests on estimated marginal means (EMMs). For graphical representation, results were back-transformed to the original scale using the corresponding inverse functions and displayed as EMM plots.

The temporal dynamics of the soil bacterial community structure were examined at the order level, focusing on the ten most abundant taxa. Principal Component Analysis (PCA) was used to explore relationships among soil properties, pedoclimatic factors, and these ten dominant bacterial orders (prcomp function). For pedoclimatic variables, mean values from the two days preceding each sampling event were used. Linear mixed models with plot as a random effect (lme function) were then applied to assess the influence of environmental factors on bacterial orders. Among the pedological and climatic variables, significant predictors were first identified through stepwise model selection (stepAIC function) for each abundant order. Model assumptions were verified using Moran's I, the Shapiro–Wilk test, and diagnostic plots; when required, variables were transformed to satisfy normality and homoscedasticity of residuals. Model performance and accuracy were evaluated using marginal and conditional R^2 values and the Akaike Information Criterion.

3. Results

3.1. Pedoclimatic Factors

3.1.1. Soil Temperature

Temperature differences were detected between sealed and unsealed soils at a depth of 30 cm (Figure 2). Overall, the de-sealed plots maintained cooler soil temperatures than both sealed positions, with an annual mean of 15.9 °C (Table 1). Seasonal analysis showed a strong cooling effect during summer (−7.2/−5.9 °C compared to S1 and S2, respectively; Cliff's $|\delta| > 0.474$). Medium to small effects were observed in spring, while in winter temperatures remained relatively uniform across cover conditions, with occasional thermal reversals (Figure 2; Table 2). In general, de-sealing increased daily temperature fluctuations, especially during extreme weather events, yet reduced seasonal thermal extremes compared to sealed soils, producing lower summer and higher winter temperatures. Temperature differences between the sealed positions were negligible in autumn and winter, and small in spring and summer, with S2 consistently cooler than S1, indicating a temperature gradient across the sealing conditions.

Temperature profiles of the unsealed soil at 10 and 30 cm depths followed similar overall trends (Figure 2), though diurnal and seasonal variability was more pronounced at 10 cm, reflecting the greater sensitivity of surface layers to meteorological conditions.

Analysis of treatment effects in the de-sealed plots showed that compost addition and vegetation type had no significant influence on soil temperature (Cliff's $|\delta| < 0.147$; Table 3).

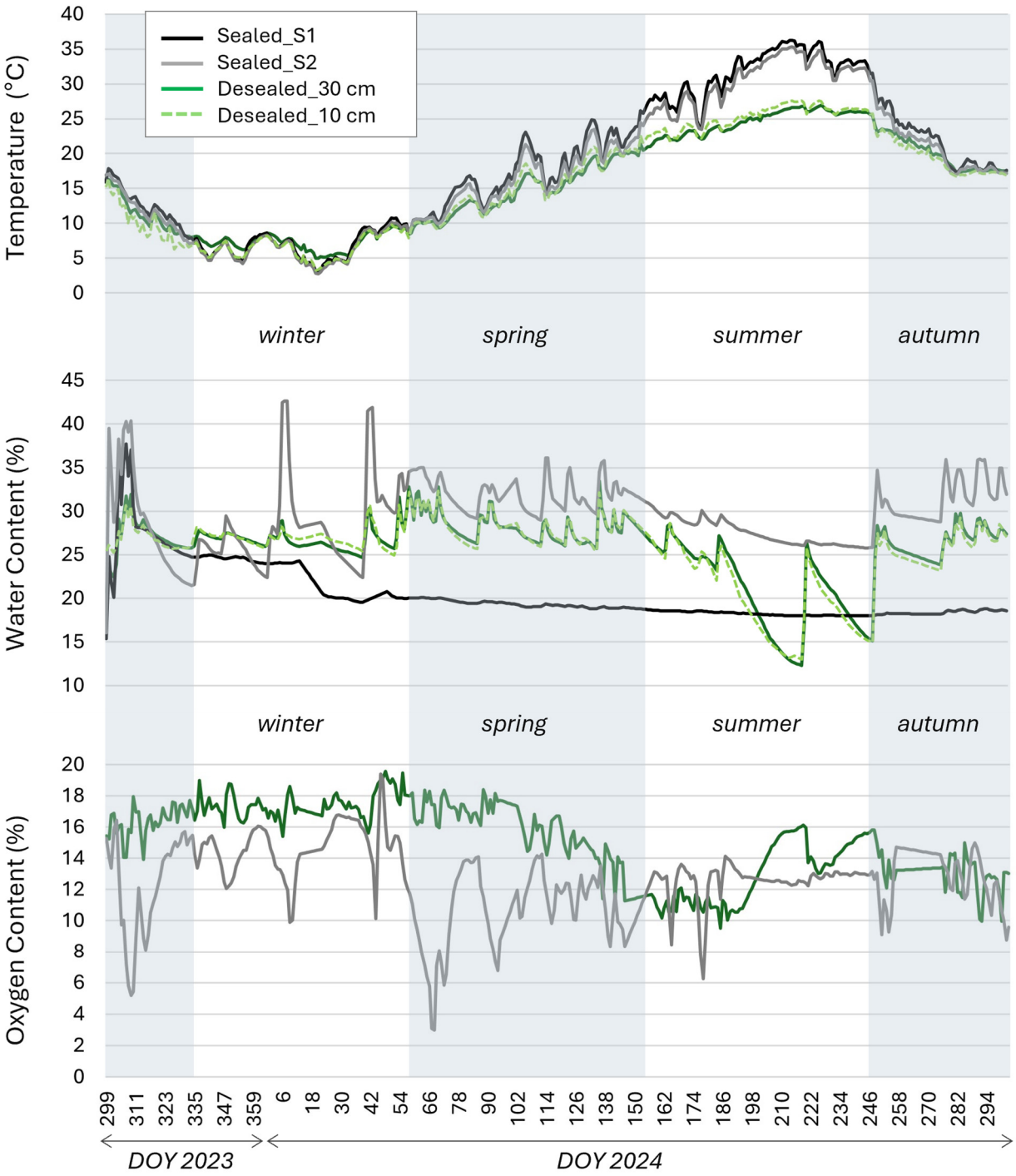

Figure 2. Pedoclimatic parameters curves during the monitoring period, divided by soil cover groups and de-sealed soil depth.

Table 1. Seasonal and annual average values (mean ± sd) of pedoclimate parameters divided by soil cover groups (D = de-sealed; S1 = well sealed; S2 = partially sealed). For the de-sealed soil the mean values were calculated as the average of the experimental plots at 10 (D_{10}) and 30 cm (D_{30}).

Parameter	Period	D_{10}	D_{30}	S1	S2
T (°C)	Winter	6.6 ± 1.7	7.3 ± 1.3	6.9 ± 2	6.6 ± 2
	Spring	15.2 ± 3.6	14.8 ± 3.3	17.5 ± 4.3	16.5 ± 3.9
	Summer	25.1 ± 1.8	24.4 ± 1.8	31.6 ± 3.4	30.4 ± 3.5
	Autumn	16 ± 5.6	16.9 ± 5.2	18.6 ± 6.2	17.8 ± 6
	Annual	15.7 ± 7.4	15.9 ± 6.9	18.7 ± 9.7	17.8 ± 9.4
SWC (%)	Winter	27.1 ± 1.3	26.8 ± 1.4	22.4 ± 2.1	28.4 ± 4.9
	Spring	28.2 ± 1.7	28.2 ± 1.7	19.3 ± 0.4	31.9 ± 1.8
	Summer	20.8 ± 4.7	21.5 ± 4.7	18.3 ± 0.2	27.8 ± 1.6
	Autumn	25.8 ± 2.8	26.4 ± 2.9	21.8 ± 5.2	30.1 ± 4.4
	Annual	25.5 ± 4	25.7 ± 3.9	20.4 ± 3.3	29.6 ± 3.9
O_2 (%)	Winter	-	17.4 ± 0.9	1 *	14.5 ± 1.8
	Spring	-	15.7 ± 1.9	1 *	10.6 ± 2.4
	Summer	-	12.8 ± 1.9	1 *	12.5 ± 1.2
	Autumn	-	14.3 ± 1.9	1 *	12.6 ± 2.4
	Annual	-	15.1 ± 2.4	1 *	12.6 ± 2.4

* Theoretical oxygen concentration based on literature values were used.

Table 2. Seasonal and annual effect size and Cliff's delta (δ) values across the soil cover groups. Cliff's δ interpretation: negligible ($|\delta| < 0.147$), small ($0.147 \leq |\delta| < 0.330$), medium ($0.330 \leq |\delta| < 0.474$) and large ($|\delta| \geq 0.474$).

Parameter	Period	D_{30}—S1			D_{30}—S2			S2—S1		
		Effect Size	Cliff's δ	Interpretation	Effect Size	Cliff's δ	Interpretation	Effect Size	Cliff's δ	Interpretation
T (°C)	Winter	0.4	0.139	Negligible	0.8	0.235	Small	−0.3	−0.104	Negligible
	Spring	−2.7	−0.359	Medium	−1.7	−0.251	Small	−1	−0.149	Small
	Summer	−7.2	−0.932	Large	−5.9	−0.829	Large	−1.2	−0.220	Small
	Autumn	−1.7	−0.145	Negligible	−0.9	−0.057	Negligible	−0.8	−0.097	Negligible
	Annual	−2.8	−0.144	Negligible	−1.9	−0.093	Negligible	−0.8	−0.052	Negligible
SWC (%)	Winter	4.5	0.993	Large	−1.6	−0.146	Negligible	6	0.805	Large
	Spring	8.8	1	Large	−3.8	−0.877	Large	12.6	1	Large
	Summer	3.2	0.432	Medium	−6.3	−0.845	Large	9.5	1	Large
	Autumn	4.6	0.547	Large	−3.8	−0.568	Large	8.3	0.762	Large
	Annual	5.2	0.706	Large	−3.9	−0.525	Large	9.1	0.914	Large
O_2 (%)	Winter	16.4 *	1 *	Large *	2.9	0.914	Large	13.5 *	1 *	Large *
	Spring	14.7 *	1 *	Large *	5.1	0.893	Large	9.6 *	1 *	Large *
	Summer	11.8 *	1 *	Large *	0.3	0.025	Negligible	11.5 *	1 *	Large *
	Autumn	13.3 *	1 *	Large *	1.8	0.360	Medium	11.6 *	1 *	Large *
	Annual	14.1 *	1 *	Large *	2.5	0.530	Large	11.6 *	1 *	Large *

* Theoretical oxygen concentration based on literature values were used.

Table 3. Effect size and Cliff's delta (δ) values between the treatments applied to de-sealed plots (CoA = Compost addition; VgT = Vegetation type). Cliff's delta interpretation: negligible ($|\delta| < 0.147$), small ($0.147 \leq |\delta| < 0.330$), medium ($0.330 \leq |\delta| < 0.474$) and large ($|\delta| \geq 0.474$).

Parameter	Treatment	Effect Size	Cliffs_Delta	Interpretation
T (°C)	CoA	0.1	0.019	Negligible
	VgT	−0.2	−0.031	Negligible
SWC (%)	CoA	−0.5	−0.016	Negligible
	VgT	1.2	0.057	Negligible
O_2 (%)	CoA	0.1	0.047	Negligible
	VgT	−3.9	−0.824	Large

3.1.2. Soil Water Content

The effects of de-sealing on soil water content showed clear differences among the soil cover conditions. With an annual mean of 25.7%, the SWC of de-sealed soil was 5.2% higher than that of well-sealed soil and 3.9% lower than that of partially sealed soil (Table 2). The largest contrasts were observed between S1 and S2 (Cliff's $|\delta| > 0.474$). This general pattern (S2 > D > S1) persisted throughout the monitoring period with a large effect size, although seasonal dynamics varied considerably among cover conditions, largely due to differing water content responses to rainfall events (Figure 2).

De-sealed soils were strongly influenced by meteorological drivers, showing the lowest SWC values in summer (Table 1; Figure 2) under drought and high-temperature conditions. Partially sealed soils (S2) responded most strongly to rainfall, reaching the highest water content values after heavy precipitation events (>15 mm), with water content levels remaining elevated longer than in unsealed plots (Figure 2). However, S2 was less affected by extreme summer drought. In contrast, the well-sealed soil (S1) exhibited a gradual, steady decline in water content that was largely independent of meteorological conditions.

In the unsealed plots, vertical profiles showed similar SWC patterns at 10 cm and 30 cm depths, with greater fluctuations in the surface layer (Figure 2). Analysis of compost addition (CoA) and vegetation type (VgT) treatments indicated negligible effects on unsealed soil water content (Cliff's $|\delta| < 0.147$; Table 3).

3.1.3. Oxygen Content in Soil Air

A marked increase in oxygen availability was recorded in the de-sealed plots compared with the sealed soils. Relative to S1, which, according to the literature, had a theoretical oxygen concentration of 1% v/v [22–24], de-sealing resulted in a clear shift from anaerobic to aerobic conditions (absolute difference +14.1%; Cliff's $\delta = 1$). A large effect was also detected relative to S2 (absolute difference +2.5%; Cliff's $|\delta| > 0.474$), although S2 was already under aerobic conditions (Table 2). A similarly large difference was found between S1 and S2 (Cliff's $\delta = 1$). The only deviation from this general pattern (D > S2 > S1) occurred at the onset of summer, when O_2 concentration in the de-sealed soil dropped markedly, falling below that of S2 (Figure 2; Table 1).

Treatment analysis showed that vegetation type had a strong effect on soil oxygen concentration (Cliff's $\delta = -0.824$), with mixed grass plots maintaining higher O_2 levels than sorghum monoculture plots (Table 3). In contrast, compost application had no significant effect.

3.2. Soil Properties

At time zero (October 2023), the unsealed soil collected from the 30 cm layer immediately beneath the RA cover showed a pH range of 6.7–7.2, organic carbon content between 0.43% and 0.55%, total nitrogen between 0.05% and 0.06%, and a C:N ratio of 7.8–8.7. Over the following year, pH exhibited a non-linear trend: starting from neutral values in October, it rose in November after RA deposition, returned to neutrality in spring, increased again in summer, and finally declined to 7.2 in autumn (Figure 3). Although not statistically significant, similar seasonal oscillations were observed in $CaCO_3$ content.

Organic carbon and total nitrogen both increased during the monitoring period, but differences among sampling dates were not significant. However, the C:N ratio indicated that t_0 and t_2 differed significantly from t_5, when higher SOC and lower nitrogen levels produced a marked rise in the C:N ratio.

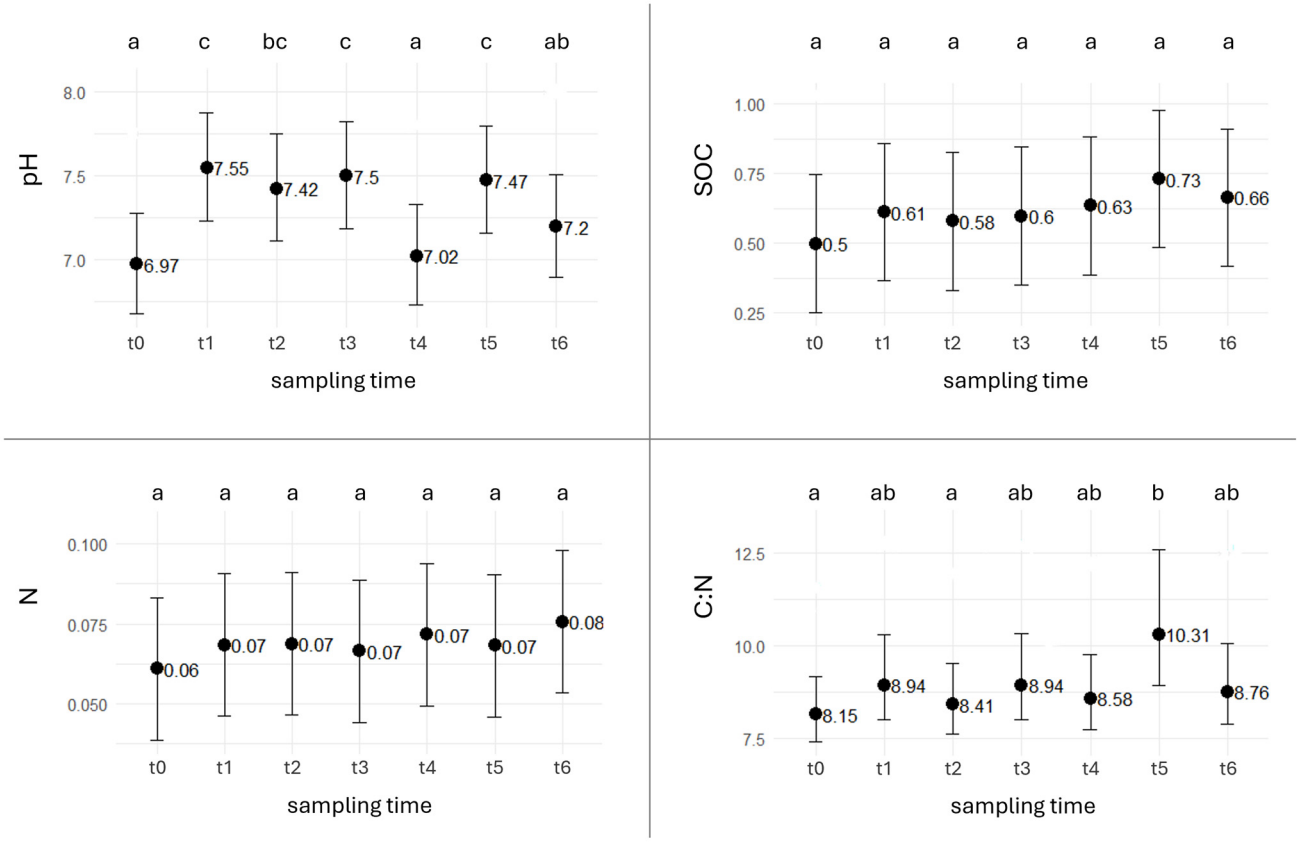

Figure 3. Plots of estimated marginal means (EMMs). Evolution of soil characteristics during time. Different letters indicate statistically significant differences. (SOC = soil organic carbon; N = total nitrogen; C:N = organic carbon to total nitrogen ratio).

3.3. Percolation Water

Metal concentrations in percolation water collected from the lysimeters are reported in Table 4. Control values, representing leachate from unsealed soil, were generally low for Pb, Cu, Ni, Cr, and Zn, with the only exceptions being Pb on 7 March 2024 (0.24 mg L^{-1}) and Ni on 6 November 2023 (0.09 mg L^{-1}).

The net metal release from the RA layer, calculated as the difference between the mean concentrations in percolation water from the four experimental plots and the corresponding control values, was also generally low. The highest releases occurred for Pb (0.14 ± 0.13 mg L^{-1}) and Ni (0.13 ± 0.06 mg L^{-1}) at the first sampling. Afterward, RA-derived contributions decreased for all monitored metals, approaching zero by the final sampling date ($\leq 0.01 \pm 0.01$ mg L^{-1}).

Table 4. Metal concentrations in percolation water: control values and mean net release from the RA layer.

Sampling Days	Control Values (mg L^{-1})					From RAs (mg L^{-1})				
	Pb	Cu	Ni	Cr	Zn	Pb	Cu	Ni	Cr	Zn
6 November 2023	0.07	0.03	0.09	0.00	0.02	0.14 ± 0.13	0.03 ± 0.02	0.13 ± 0.06	0.00 ± 0.00	0.02 ± 0.00
31 January 2024	0.06	0.01	0.03	0.00	0.01	0.02 ± 0.02	0.07 ± 0.04	0.09 ± 0.08	0.00 ± 0.00	0.02 ± 0.03
7 March 2024	0.24	0.04	0.02	0.06	0.01	−0.03 ± 0.05	0.03 ± 0.02	0.03 ± 0.06	0.02 ± 0.02	0.03 ± 0.05
11 April 2024	0.00	0.04	0.04	0.04	0.02	0.00 ± 0.00	0.03 ± 0.02	0.05 ± 0.06	0.00 ± 0.01	0.02 ± 0.04
08 May 2024	0.00	0.04	0.06	0.03	0.02	0.00 ± 0.00	0.03 ± 0.02	0.05 ± 0.05	0.00 ± 0.01	0.00 ± 0.01
05 June 2024	0.00	0.04	0.04	0.00	0.01	0.00 ± 0.00	0.03 ± 0.02	0.05 ± 0.03	0.00 ± 0.00	0.02 ± 0.03
24 July 2024	0.00	0.03	0.05	0.00	0.01	0.00 ± 0.00	0.01 ± 0.01	0.01 ± 0.01	0.00 ± 0.00	0.00 ± 0.01

3.4. Bacterial Community Composition

After quality filtering and removal of non-bacterial ASVs, a total of 521,131 sequences were obtained, ranging from 1355 to 96,265 per sample. Data from three samples (D1 in April 2024, D3 in July 2024, and D4 in October 2024) were unavailable due to accidental loss.

Characterisation of the bacterial community showed that much of the soil diversity remains unknown: 72% of ASVs were unclassified at the genus level, and 47% at the order level. Caryophanales and Gemmatimonadales were the most abundant orders across all experimental plots throughout the year, followed by Micromonosporales and Hyphomicrobiales (Figure 4).

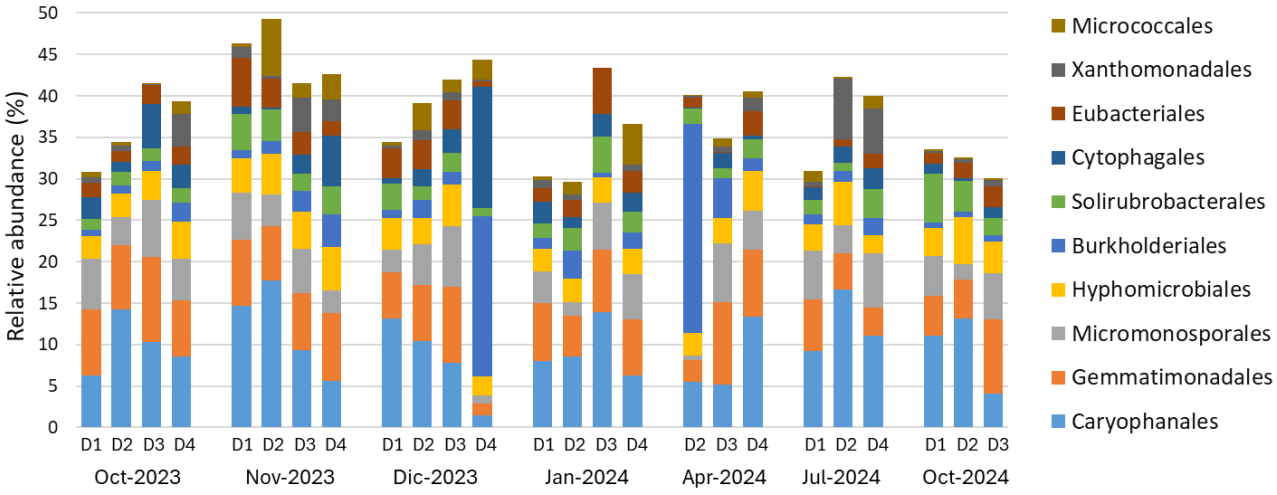

Figure 4. Relative abundance of the ten most abundant bacterial orders. D1, D2, D3 and D4 represent the experimental plots. Due to accidental reasons, data from D1 in April 2024, D3 in July 2024 and D4 in October 2024 are missing.

Occasional plot-specific differences appeared in December 2023 and April 2024, when D4 and D2, respectively, showed higher abundances of Burkholderiales (and Cytophagales in D4) compared with other samples, including those from the same plots at other times. Overall, no consistent temporal trends or clear spatial differentiation among plots were observed.

3.5. Soil, Pedoclimate and Bacterial Communities

The first two principal components of the PCA (Figure 5a) accounted for 40.9% of the total variance (PC1: 22.7%, PC2: 18.2%). As shown in Figure 5b, SOC and the C:N ratio were the main drivers of PC1 and PC2, followed by SWC and N. In contrast, pH, T, and O_2 mainly contributed to the third component (PC3), which explained an additional 16.6% of the variance. The PCA plot indicates that SOC and the C:N ratio were positively correlated with pH and temperature. Regarding bacterial orders, Xanthomonadales were closely associated with high SOC, high C:N ratios, and elevated T, while Gemmatimonadales, Micromonosporales, and Eubacteriales correlated positively with SWC and O_2.

Linear mixed model results (Table 5) showed that Hyphomicrobiales abundance was significantly influenced by SOC, N, and the C:N ratio. Soil pH affected only Gemmatimonadales, whereas carbonate content influenced Eubacteriales and Micrococcales. Among pedoclimatic factors, T significantly affected only Eubacteriales, and SWC affected Xanthomonadales, while no significant relationships were observed with O_2. Finally, Solirubrobacterales and Micrococcales were the only orders significantly affected by 'days after de-sealing,' with the abundance of Micrococcales further influenced by N.

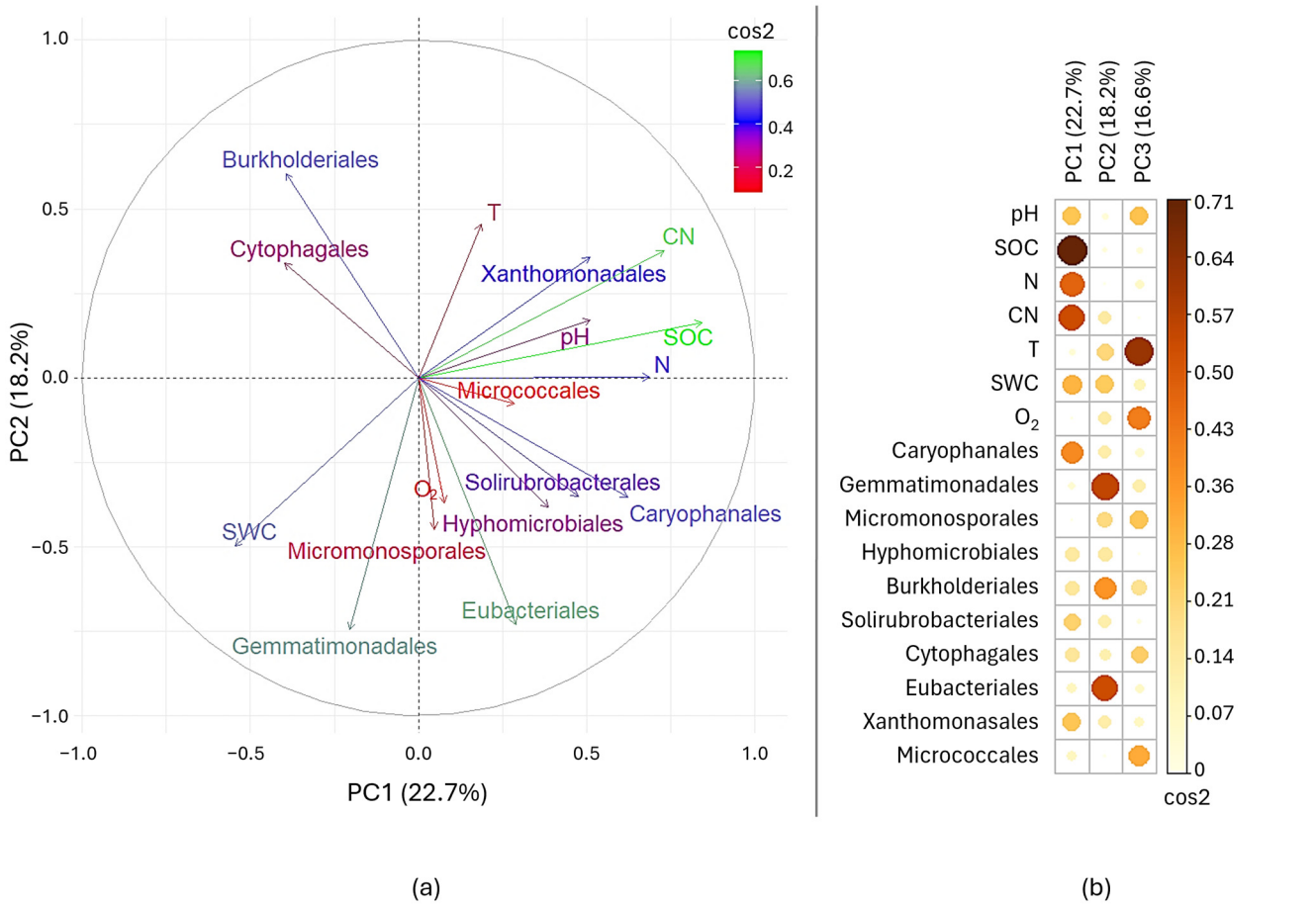

Figure 5. (**a**) PCA showing the relationships among the ten most abundant bacterial orders, pedoclimatic factors (T, SWC, O_2) and soil properties (pH, SOC, N, C:N). (**b**) Quality of representation (cos2) of each variable to PC1, PC2 and PC3 separately.

Table 5. Results of linear mixed models: *p*-values of the significant predictors (previously selected for each order with the stepwise model) that affected the abundance of bacterial orders. R^2m and R^2c are respectively the marginal and the conditional R-squared of each model. R^2m represents the variance explained by fixed effect only, while R^2c represents the variance explained by both the fixed and random effects.

Order	Day	pH	$CaCO_3$	SOC	N	CN	T	SWC	O2	R^2m	R^2c
Caryophanales					0.059					0.14	0.31
Gemmatimonadales		0.031 *								0.22	0.47
Micromonosporales				0.374		0.732				0.05	0.57
Hyphomicrobiales				0.020 *	0.016 *	0.031 *	0.051		0.098	0.35	0.35
Burkholderiales				0.097						0.09	0.49
Xanthomonadales	0.103	0.207					0.113	0.011 *		0.52	0.52
Solirubrobacterales	0.015 *						0.055			0.25	0.25
Cytophagales			0.052			0.065		0.070	0.257	0.19	0.39
Eubacteriales			0.049 *				0.002 *			0.38	0.38
Micrococcales	0.023 *		0.003 *		0.012 *					0.47	0.47

* *p*-values statistically significant.

4. Discussion

4.1. De-Sealing Effects on Pedoclimate Factors

This experiment demonstrated that de-sealing strongly affected the soil microclimate. Unsealed soils showed lower mean temperatures than sealed soils, particularly during summer. This difference results from the warming effect of impervious surfaces, which retain more radiation and accumulate more heat than bare soil [28]. Removing the pavement restores direct soil–atmosphere heat exchange and allows dissipation through conduction, evaporation, and, once vegetation is established, evapotranspiration. The improved heat exchange in de-sealed soil was evident in two ways: larger daily temperature fluctuations, reflecting responsiveness to meteorological conditions, and reduced seasonal thermal extremes. Seasonal thermal buffering is especially important in summer, when de-sealed soils maintained temperatures around 24–25 °C (mean values at 10 cm and 30 cm depth, respectively), compared with 30–31 °C in sealed soils (mean values at 30 cm depth in S2 and S1, respectively). Since lower soil temperatures help reduce surface air temperatures, these differences are relevant for mitigating the urban heat island effect.

Soil water content dynamics showed that de-sealing enhances water infiltration and regulation. At the same time, unsealed soils were more vulnerable to summer drought, confirming their strong response to meteorological drivers. In this study, partially sealed soils exhibited the highest water content and retention. This pattern likely reflects water infiltration through pavement cracks or preferential pathways that redirect lateral rainfall, leading to localised water accumulation under the sealed layer, where water loss occurs mainly through limited evaporation [29,30]. By contrast, water content in well-sealed soils decreased gradually and independently of rainfall or weather conditions, demonstrating that these soils cannot receive or store rainwater and thus cannot contribute to water regulation functions [31,32]. De-sealing therefore plays a key role in restoring soil water regulation by reestablishing exchanges between the pedosphere, biosphere, and atmosphere.

Due to the malfunction of the S1 oxygen sensor, a literature-based value of 1% [22–24] was used to model a perfectly sealed soil scenario. Other studies have reported oxygen concentrations beneath pavements of 2–5% [33,34], reflecting the many factors influencing soil oxygen, including temperature, water content, texture, compaction, respiration, pavement type, and sealing conditions [30]. It is possible that actual oxygen in S1 exceeded 1%. However, the very large effect size (Cliff's $\delta = 1.0$) between de-sealed and S1 indicates that even if S1 oxygen ranged from 2–5%, de-sealed soils would still show substantially

higher oxygen availability. The exact magnitude of the increase remains uncertain, with reliable observations limited to comparisons between de-sealed (D) and partially sealed (S2) soils. Significantly higher oxygen in de-sealed soils confirmed that de-sealing restores more aerobic conditions. Enhanced aeration, in turn, supports microbial activity, root respiration, and nutrient cycling, all of which improve soil quality and function.

Despite this increase, a temporary seasonal decline in soil oxygen occurred in de-sealed plots during summer, likely due to higher temperatures promoting microbial and root respiration [35,36]. Oxygen levels in de-sealed soils were also influenced by vegetation: mixed grasslands consistently showed higher oxygen content than sorghum monocultures, reflecting the effects of root morphology and chemistry on respiration and aeration [37]. Experimental treatments in de-sealed plots had no significant effects on soil temperature or water content.

Our observations of summer cooling and enhanced soil water content regulation are consistent with other Italian studies on permeable pavements, which reported surface temperature reductions of 3–5 °C and improved infiltration compared with impervious layers [30]. Unlike most previous work, which focused on surface conditions, our monitoring at multiple soil depths and continuous oxygen assessment provides novel insights.

4.2. Temporal Changes in Soil Properties and RA Effects

While de-sealing immediately affected the soil microclimate, no significant changes in soil properties were observed over the year, reflecting the slow pace of pedogenesis. Small increases in organic carbon, total nitrogen, and cation exchange capacity were recorded, indicating a gradual accumulation of organic matter and enhanced soil buffering. The C:N ratio showed a significant increase in July 2024, likely driven by seasonal inputs of plant residues, roots, and exudates, or by varying decomposition rates mediated by microbial communities [38]. These findings align with the slow pedogenesis reported by Maienza et al. (2021) [6], who observed notable improvements in soil chemical properties 2–3 years after de-sealing. Similarly, Renella (2020) [12] found that microbial activity responded within 6–12 months, while chemical properties remained largely stable during the first year. Together, these studies suggest that biological recovery may precede chemical changes, with 1–2 years representing an early stage in a multi-year restoration trajectory.

Soil pH and carbonate content fluctuated seasonally, likely due to a combination of chemical leaching from RAs and ion accumulation. Concrete-based RAs release alkaline substances, such as calcium hydroxide ($Ca(OH)_2$) and calcium carbonate ($CaCO_3$). Early in the experiment, soil water content and percolating water promoted the dissolution of calcium oxides and hydroxides [39], releasing OH^- ions and temporarily increasing pH. Over time, dissolution and carbonation consumed these reactive compounds, while the less soluble $CaCO_3$ acted as a buffer, moving pH closer to neutrality [39,40]. During summer, higher temperatures and lower water content reduced ion leaching and promoted soluble salt accumulation, causing pH to rise again. Although microbial respiration likely increased with temperature, as suggested by declining O_2 levels and presumably higher CO_2 production, the potential acidifying effect of microbial activity was likely outweighed by the buffering capacity of carbonates and basic cations. Root activity and exudates may also have contributed to summer pH fluctuations, but differences among vegetation–compost combinations and the lack of plot replicates prevented quantitative assessment. Autumn rainfall then likely flushed accumulated bases, returning pH to near-neutral values.

Monitoring of metals in percolation water showed only minimal release of Pb and Ni at the start of the experiment. These metals can originate from various components of construction and demolition waste, including plaster, mortar, ceramics, and red bricks

within the RAs [41–43]. Their concentrations declined over time to levels comparable with control soil, indicating that RA application did not compromise percolation water quality.

Overall, no adverse effects of RAs, such as excessive alkalinization with reduced nutrient availability and biological activity, heavy metal contamination, or phytotoxicity, were observed. pH remained within a neutral to slightly alkaline range (7.0–7.6), suitable for most biological processes. Heavy metal release was minimal and transient, decreasing to control levels within months. Organic matter increased gradually, bacterial communities showed no signs of stress or compositional collapse due to RAs, and vegetation established successfully without nutrient deficiency or toxicity symptoms.

Nevertheless, the chemical and physical properties of RAs can vary depending on source materials and production methods. This variability may influence the release of pollutants, trace elements, and emerging contaminants. Further research is needed to evaluate the chemical behaviour and long-term environmental risks of different RA types.

4.3. Bacterial Community Composition and Evolution

The high percentage of unclassified taxa observed in the bacterial communities highlighted the still limited knowledge of soil biodiversity [13]. Overall, bacterial orders from Pseudomonadota (29.3 ± 6.6%), Actinomycetota (17.5 ± 4.7%) and Bacillota (13.1 ± 5.1%) phyla were dominant. They are ubiquitous in soils and known to be involved in the degradation of organic matter and carbon cycling processes [44].

The overall impact of the de-sealing intervention on bacterial community evolution was limited, since no major trends could be observed. Particularly, the high abundance of several subdominant orders of the Actinomycetota phylum, such as Micromonosporales and Solirubrobacterales, which is known to be mainly represented by aerobic members [44], indicates an overall prevalence of aerobic metabolisms. Notably, linear mixed models indicated that none of the most abundant orders was significantly affected by the soil oxygen content, and only two of them were significantly influenced by the 'days after de-sealing'. The lack of a significant relationship with soil oxygen and time since de-sealing may reflect the fact that the soil was already in aerobic conditions at the beginning of the experiment, at least partially. The co-occurrence of several orders of aerobic Actinomycetota and of typically anaerobic bacteria, such as the order Eubacteriales and members of the class Deltaproteobacteria, mainly unclassified, may suggest the existence of mixed aerobic/anaerobic conditions [44]. This could be due to a rapid increase in oxygen concentrations and microbial activity occurring within the first 48 h after de-sealing (time prior to the initial sampling) or, more likely, to uncomplete sealing conditions, which allowed the soil to maintain relatively high oxygen levels, similar to those observed in the partially sealed soil (S2), even before the de-sealing intervention. The absence of a clear temporal trend in bacterial community evolution, despite the observed fluctuations in pH and C:N ratio values, may indicate the occurrence of a relatively stable and robust community, already ecologically adapted to local soil conditions. Prolonged monitoring will be essential to highlight possible shifts due to the long-term effects of de-sealing and/or the different experimental treatments applied.

During the monitored period, a few differences in bacterial community composition were observed among the de-sealed plots, but apparently not related to seasonality or to the different experimental treatments. In contrast, the Principal Component Analysis (PCA) highlighted that the distribution of bacterial orders was strongly influenced by pedological and climatic variables. The variables that drove the major differences in bacterial community composition were SOC and the C:N ratio, followed by soil water content and total nitrogen. This is in contrast with literature, which often indicates pH as the main factor influencing bacterial community structure in soils [13,45]. However,

although pH and soil temperature contributed only marginally to the first two principal components, they showed a positive correlation with C:N ratio and SOC, suggesting a possible combined effect on bacterial community structure. In addition, linear mixed models confirmed that the most abundant bacterial orders varied more according to soil characteristics than to pedoclimatic factors.

Such dependence may be regarded as a proxy of a differential involvement of the main bacterial populations in soil biogeochemical cycles. Particularly, Hyphomicrobiales were positively correlated with SOC, C:N ratio and total nitrogen content. Members of this order are nitrogen fixers and can establish endosymbiotic nitrogen fixation relationships with leguminous roots [46,47]. Their increased abundance can therefore be considered as a proxy of increased soil functionality, since they can boost both carbon and nitrogen cycles. Micrococcales were positively correlated to total nitrogen and $CaCO_3$ content, while Gemmatimonadales were negatively correlated with pH. The abundance of the latter has already been shown to be constrained by pH values diverging from neutrality [48]. Due to their active involvement in carbon and nitrogen cycling, both orders are commonly regarded as indicators of soil multifunctionality, and they are generally enriched under appropriate agronomic practices [49–51]. All together, these results suggest that many of the dominant bacterial populations in soils are actively involved in key soil functions, such as carbon storage and nitrogen fixation, and their relative abundance may be modulated by fluctuations in soil properties. Therefore, after a de-sealing intervention, monitoring of such parameters is essential to timely observe the onset of environmental conditions that could impair microbial activity, thus reducing the targeted soil functional recovery. Particularly, it is crucial to monitor pH shifts, since abrupt and strong pH increases may rapidly lead to a depletion of key microbial taxa with consequent loss of soil functions.

Although apparently less impacting on bacterial populations than soil characteristics, pedoclimatic factors, and especially SWC, also played a role in bacterial community assembly. In fact, the dominance of drought tolerant and oligotrophic orders (Caryophanales, mainly represented by families Bacillaceae and Paenibacillaceae, and Gemmatimonadales) aligns with the sandy, relatively nutrient-poor soil and dry summer conditions [48,52,53]. Furthermore, the abundance of Xanthomonadales, mainly belonging to genera *Lysobacter* and *Arenimonas*, was negatively related to soil water content. Several species of *Arenimonas* were previously isolated from saline and alkaline soils [54,55], and their abundance was increased under mixed irrigation with brackish and reclaimed water [56]. Members of genus *Lysobacter* are generally able to produce a wide range of metabolites with activity against other bacteria, fungi and nematodes, and were found to be particularly abundant in disease suppressive soils [57]. Therefore, members of this order may have the ability to cope with stress conditions, especially due to drought, alkalinity, and the presence of plant pathogens, thus contributing to improving soil properties.

5. Conclusions

This study provides one of the most comprehensive assessments of de-sealing outcomes conducted in Europe, addressing critical knowledge gaps. Although direct comparisons with other European projects are limited by the scarcity of soil-focused field studies, our results align with the available evidence. Pedoclimatic improvements, such as enhanced soil aeration, water regulation, and heat exchange capacity, occurred rapidly after de-sealing, creating favourable microclimatic conditions for biological activity.

Our integrated assessment, which documented pH dynamics, metal leaching, soil property changes, and bacterial community responses, also shows that properly characterised concrete-based RAs do not hinder soil restoration in field conditions. At the same time, their use supports circular economy practices by reducing both economic and environ-

mental costs. The minimal pH fluctuations, transient and minor metal release, maintained bacterial diversity, and successful vegetation establishment collectively demonstrated the environmental safety of this approach. However, the effects of RAs on soil and water depend strongly on their composition and the environmental context. Therefore, our findings are representative of the specific experimental site and the RA type used.

The relatively short monitoring period did not capture long-term cumulative effects of de-sealing and RA addition. Pedoclimatic improvements appear structurally stable, but chemical and biological soil development occurs over multiple years or decades. Metal release from RAs is expected to remain low under alkaline conditions, yet uncertainties remain regarding their long-term chemical behaviour and degradation pathways. Multi-year monitoring (5–10 years) that integrates pedoclimate, chemistry, microbial and faunal communities, vegetation, and leachate is essential to confirm these preliminary findings and to disentangle the effects of seasonal fluctuations from those induced by de-sealing and RA addition.

The limited comparability across European de-sealing projects highlights the need for coordinated research with standardised monitoring protocols and common indicators. Such harmonisation would allow systematic comparisons across sites, climates, RA types, and management practices. The resulting evidence could then be used to optimise de-sealing and restoration strategies, promoting soil development and functional recovery more effectively.

Supplementary Materials: The following supporting information can be downloaded at: https://www.mdpi.com/article/10.3390/soilsystems9040128/s1, Figure S1: Pedological profile P2 in the study area; Figure S2: Relative abundance (%) of the ten most abundant bacterial orders; Table S1: Main characteristics of the pedological profiles; Table S2: Methods and results of the leaching test performed on the recycles aggregates.

Author Contributions: Conceptualization, G.M., R.C. and C.F.; data curation, G.M., R.C., I.G. and C.F.; formal analysis, G.M., R.C., F.P. and I.G.; investigation, G.M., R.C. and C.F.; methodology, G.M., R.C. and C.F.; project administration, G.M., R.C. and C.F.; resources, G.M., I.G. and C.F.; software, R.C.; supervision, C.F.; validation, R.C.; visualization, G.M. and R.C.; writing—original draft, G.M.; writing—review & editing, G.M., R.C., F.P., I.G. and C.F. All authors have read and agreed to the published version of the manuscript.

Funding: This research was partially funded by the National Recovery and Resilience Plan (NRRP), Mission 4 Component 2 Investment 1.4—Call for tender No. 3138 of 16 December 2021, rectified by Decree n.3175 of 18 December 2021 of Italian Ministry of University and Research funded by the European Union—NextGenerationEU. Award Number: Project code CN_00000033, Concession Decree No. 1034 of 17 June 2022 adopted by the Italian Ministry of University and Research, CUP H43C22000530001, Project title "National Biodiversity Future Center—NBFC.

Institutional Review Board Statement: Not applicable.

Informed Consent Statement: Not applicable.

Data Availability Statement: Raw DNA sequences were submitted to Sequence Read Archive (SRA-NCBI), with accession numbers SAMN52863942-SAMN52863978, BioProjects PRJNA1347647 (Submission ID: SUB15724367, release date: 15 November 2025) and PRJNA1108077. Other raw data supporting the conclusions of this article will be made available by the authors on request.

Acknowledgments: The authors would like to thank the Centro Forestazione Urbana of the Italia Nostra Milano Nord association, which managed the Parco di Porto di Mare area, for technical and financial support in the de-sealing operations, as well as in the management of demolition waste and recycled aggregates.

Conflicts of Interest: The authors declare no conflicts of interest.

Appendix A. Sensor Data Processing

TEROS 11 sensors use a thermistor to measure temperature [°C]. The measurement is optimised to be accurate when the sensor is fully buried in soil and the value does not need to be converted or corrected. The same sensors use an electromagnetic field to measure the dielectric permittivity of the soil, i.e., the ability of soil to hold an electric charge, strictly linked to the soil water content. The raw value of dielectric permittivity (RAW) is then converted to percentage volumetric soil water content (SWC) by the following calibration equation for mineral soil:

$$SWC = (3.879 \times 10^{-4} \times RAW - 0.6956) \times 100 \quad (A1)$$

Apogee SO-110 series oxygen sensors are galvanic cell type sensors. They operate by electrochemical reaction of oxygen with an electrolyte, which consumes a small amount of oxygen and produces an electrical current. The output is an analogue voltage that is linearly proportional to the absolute oxygen concentration. A linear function is used to derive a calibration factor and convert voltage output to the oxygen partial pressure:

$$O_{2m} = CF \times mV_m - Offset \quad (A2)$$

$$CF = (0.2095 \times PB)/(mVC - mV_0) \quad (A3)$$

where O_{2m} is the partial pressure of oxygen measured [kPa], CF the calibration factor [kPa(O_2)/mV], mV_m the measured voltage output [mV], and the sensor Offset is calculated by multiplying CF by mV_0, which is the voltage output under zero oxygen condition (O_2 = 0 kPa O_2; $mV_0 = 3 \pm 2$ mV). The mV_C is the voltage output during the onsite calibration [mV] and P_B is the barometric pressure [kPa] (0.2095 multiplied by P_B equals partial pressure of oxygen under ambient conditions). The calibration was performed by placing the sensor over water in sealed chamber, with ambient air filling the headspace. This setup simulated a 100% humidity environment and represented the recommended calibration procedure for measurements in soils.

However, sensor electronics are affected by temperature; thus, an empirical correction derived from measured data must be applied to the partial pressure of oxygen measured:

$$O_2 = O_{2m} + C_3 \times {T_S}^3 + C_2 \times {T_S}^2 + C_1 \times T_S + C_0 \quad (A4)$$

$$C_0 = -(C_3 \times {T_C}^3 + C_2 \times {T_C}^2 + C_1 \times T_C) \quad (A5)$$

where T_S is the temperature measured by the sensor itself [°C] and T_C is the temperature measured during the calibration [°C]. C_1, C_2 and C_3 are the correction coefficients for Apogee SO-110 sensors ($C_1 = -6.949 \times 10^{-2}$; $C_2 = 1.422 \times 10^{-3}$; $C_3 = -8.213 \times 10^{-7}$).

References

1. Fabbri, D.; Pizzol, R.; Calza, P.; Malandrino, M.; Gaggero, E.; Padoan, E.; Ajmone-Marsan, F. Constructed Technosols: A Strategy toward a Circular Economy. *Appl. Sci.* **2021**, *11*, 3432. [CrossRef]
2. European Environment Agency. *The European Environment—State and Outlook 2020—Knowledge for Transition to a Sustainable Europe*; Publications Office: Luxembourg, 2019; ISBN 9789294800909.
3. European Commission and Directorate-General for Environment. *Guidelines on Best Practice to Limit, Mitigate or Compensate Soil Sealing*; Publications Office: Luxembourg, 2012.
4. European Commission; Veerman, C.; Pinto Correia, T.; Bastioli, C.; Biro, B.; Bouma, J.; Cienciala, E.; Emmett, B.; Frison, E.A.; Grand, A.; et al. *Caring for Soil Is Caring for Life—Ensure 75% of Soils Are Healthy by 2030 for Food, People, Nature and Climate—Report of the Mission Board for Soil Health and Food*; Publications Office: Luxembourg, 2020; ISBN 9789276216032.
5. Tobias, S.; Conen, F.; Duss, A.; Wenzel, L.M.; Buser, C.; Alewell, C. Soil Sealing and Unsealing: State of the Art and Examples. *Land Degrad. Dev.* **2018**, *29*, 2015–2024. [CrossRef]

6. Maienza, A.; Ungaro, F.; Baronti, S.; Colzi, I.; Giagnoni, L.; Gonnelli, C.; Renella, G.; Ugolini, F.; Calzolari, C. Biological Restoration of Urban Soils after De-Sealing Interventions. *Agriculture* **2021**, *11*, 190. [CrossRef]
7. Vieillard, C.; Vidal-Beaudet, L.; Dagois, R.; Lothode, M.; Vadepied, F.; Gontier, M.; Schwartz, C.; Ouvrard, S. Impacts of Soil De-Sealing Practices on Urban Land-Uses, Soil Functions and Ecosystem Services in French Cities. *Geoderma Reg.* **2024**, *38*, e00854. [CrossRef]
8. Sintesi Di Norme, Linee Guida, Buone Pratiche, Casi Studio in Materia Di Limitazione Di Consumo Di Suolo e Resilienza Urbana al Cambiamento Climatico. Azione A1.3, SOS4LIFE—Save Our Soil for Life. 2017. Available online: https://www.sos4life.it/wp-content/uploads/SOS4Life_Sintesi_norme_buone-pratiche_consumo_suolo_A.1.3-4.pdf (accessed on 19 June 2025).
9. Caselli, B.; Ceci, M.; De Noia, I.; Garda, E.; Zazzi, M. Towards the Integration of Soil Desealing in the Urban Areas' Transformation Processes. In *Innovation in Urban and Regional Planing*; Marucci, A., Zullo, F., Fiorini, L., Saganeiti, L., Eds.; Springer: Cham, Switzerland, 2024; pp. 286–298.
10. ISTAT—Istituto Nazionale Di Statistica. *Ambiente Urbano—Anno 2023*; ISTAT—Istituto Nazionale Di Statistica: Rome, Italy, 2025.
11. Aimar, F. Limiting Soil Sealing and Depaving: Local Actions for Regenerating Public Spaces to Build Green Infrastructures. In *Green Infrastructure, Planning Strategies and Environmental Design*; Giudice, B., Novarina, G., Voghera, A., Eds.; Springer: Cham, Switzerland, 2023; pp. 127–137.
12. Renella, G. Evolution of Physico-Chemical Properties, Microbial Biomass and Microbial Activity of an Urban Soil after de-Sealing. *Agriculture* **2020**, *10*, 596. [CrossRef]
13. Fierer, N. Embracing the Unknown: Disentangling the Complexities of the Soil Microbiome. *Nat. Rev. Microbiol.* **2017**, *15*, 579–590. [CrossRef]
14. Le Guern, C.; Prézeau, F.; Clozel, B.; Leduc, T.; Musy, M.; Rodler, A.; Tasca-Guernouti, S.; Béchet, B.; Dufrasnes, E.; Stabile, O.; et al. Soil Properties and Desealing Strategies: Feedback from the DésiVille Project (France). In Proceedings of the SUITMA 11 Conference on Soils of Urban, Industrial, Traffic and Mining Areas, Berlin, Germany, 5–9 September 2022.
15. Adobati, F.; Garda, E. Soil Releasing as Key to Rethink Water Spaces in Urban Planning. *City Territ. Archit.* **2020**, *7*, 9. [CrossRef]
16. European Commission. Commission Decision of 18 December 2014 Amending Decision 2000/532/EC on the List of Waste Pursuant to Directive 2008/98/EC of the European Parliament and of the Council. *Off. J. Eur. Union* **2014**, *950*, 3–24.
17. Pacheco, J.; De Brito, J.; Lamperti Tornaghi, M. *Use of Recycled Aggregates in Concrete: Opportunities for Upscaling in Europe*; Publications Office of the European Union: Luxembourg, 2023.
18. European Commission; Directorate-General for Internal Market, Industry, Entrepreneurship and SMEs. *EU Construction & Demolition Waste Management Protocol Including Guidelines for Pre-Demolition and Pre-Renovation Audits of Construction Works—Updated Edition 2024*; Publications Office of the European Union: Luxembourg, 2024.
19. Coull, M.; Butler, B.; Hough, R.; Beesley, L. A Geochemical and Agronomic Evaluation of Technosols Made from Construction and Demolition Fines Mixed with Green Waste Compost. *Agronomy* **2021**, *11*, 649. [CrossRef]
20. Morel, A.; Vidal-Beaudet, L.; Brialix, L.; Lemesle, D.; Bulot, A.; Herpin, S. Evolution of Microclimate Following Small Patch De-Sealing and Revegetation in Urban Context. *Urban Clim.* **2025**, *61*, 102371. [CrossRef]
21. IUSS Working Group WRB. *World Reference Base for Soil Resources. International Soil Classification System for Naming Soils and Creating Legends for Soil Maps*, 4th ed.; International Union of Soil Sciences (IUSS): Vienna, Austria, 2022.
22. Abreu, L.; Lutes, C.C.; Nichols, E.M. *3-D Modeling of Aerobic Biodegradation of Petroleum Vapors: Effect of Building Area Size on Oxygen Concentration Below the Slab*; EPA 510-R-13-002; EPA: Washington, DC, USA, 2013.
23. Verginelli, I.; Yao, Y.; Wang, Y.; Ma, J.; Suuberg, E.M. Estimating the Oxygenated Zone beneath Building Foundations for Petroleum Vapor Intrusion Assessment. *J. Hazard. Mater.* **2016**, *312*, 84–96. [CrossRef]
24. U.S. Environmental Protection Agency. *Technical Guide For Addressing Petroleum Vapor Intrusion at Leaking Underground Storage Tank Sites. U.S.*; EPA 510-R-15-001; EPA: Washington, DC, USA, 2015.
25. Ministro Dell'Ambiente e Della Tutela Del Territorio. Regolamento Recante Modifiche al Decreto Ministeriale 5 Febbraio 1998 Individuazione Dei Rifiuti Non Pericolosi Sottoposti Alle Procedure Semplificate Di Recupero, Ai Sensi Degli Articoli 31 e 33 Del Decreto Legislativo 5 Febbraio 1997, n. 22. D.M. 186/2006. *Gazz. Uff.* **2006**, *115*. Available online: https://www.gazzettaufficiale.it/atto/serie_generale/caricaDettaglioAtto/originario?atto.dataPubblicazioneGazzetta=2006-05-19&atto.codiceRedazionale=006G0202&elenco30giorni=false (accessed on 17 September 2025).
26. Nava, V.; Leoni, B.; Arienzo, M.M.; Hogan, Z.S.; Gandolfi, I.; Tatangelo, V.; Carlson, E.; Chea, S.; Soum, S.; Kozloski, R.; et al. Plastic Pollution Affects Ecosystem Processes Including Community Structure and Functional Traits in Large Rivers. *Water Res.* **2024**, *259*, 121849. [CrossRef]
27. Gandolfi, I.; Canedoli, C.; Rosatelli, A.; Covino, S.; Cappelletti, D.; Sebastiani, B.; Tatangelo, V.; Corengia, D.; Pittino, F.; Padoa-Schioppa, E.; et al. Microbiomes of Urban Trees: Unveiling Contributions to Atmospheric Pollution Mitigation. *Front. Microbiol.* **2024**, *15*, 1470376. [CrossRef]
28. Nwakaire, C.M.; Onn, C.C.; Yap, S.P.; Yuen, C.W.; Onodagu, P.D. Urban Heat Island Studies with Emphasis on Urban Pavements: A Review. *Sustain. Cities Soc.* **2020**, *63*, 102476. [CrossRef]

29. Nimmo, J.R. The Processes of Preferential Flow in the Unsaturated Zone. *Soil Sci. Soc. Am. J.* **2021**, *85*, 1–27. [CrossRef]
30. Fini, A.; Frangi, P.; Mori, J.; Donzelli, D.; Ferrini, F. Nature Based Solutions to Mitigate Soil Sealing in Urban Areas: Results from a 4-Year Study Comparing Permeable, Porous, and Impermeable Pavements. *Environ. Res.* **2017**, *156*, 443–454. [CrossRef] [PubMed]
31. Tóth, G.; Ivits, E.; Prokop, G.; Gregor, M.; Fons-Esteve, J.; Milego Agràs, R.; Mancosu, E. Impact of Soil Sealing on Soil Carbon Sequestration, Water Storage Potentials and Biomass Productivity in Functional Urban Areas of the European Union and the United Kingdom. *Land* **2022**, *11*, 840. [CrossRef]
32. Recanatesi, F.; Petroselli, A. Land Cover Change and Flood Risk in a Peri-Urban Environment of the Metropolitan Area of Rome (Italy). *Water Resour. Manag.* **2020**, *34*, 4399–4413. [CrossRef]
33. Morgenroth, J.; Buchan, G. Soil Moisture and Aeration Beneath Pervious and Impervious Pavements. *Arboric. Urban For.* **2009**, *35*, 135–141. [CrossRef]
34. Owens, P.R.; Wilding, L.P.; Miller, W.M.; Griffin, R.W. Using Iron Metal Rods to Infer Oxygen Status in Seasonally Saturated Soils. *CATENA* **2008**, *73*, 197–203. [CrossRef]
35. Schnecker, J.; Baldaszti, L.; Gündler, P.; Pleitner, M.; Sandén, T.; Simon, E.; Spiegel, F.; Spiegel, H.; Urbina Malo, C.; Zechmeister-Boltenstern, S.; et al. Seasonal Dynamics of Soil Microbial Growth, Respiration, Biomass, and Carbon Use Efficiency in Temperate Soils. *Geoderma* **2023**, *440*, 116693. [CrossRef]
36. Leyrer, V.; Poll, C.; Wirsching, J.; Kandeler, E.; Marhan, S. Warming Persistently Stimulates Respiration from an Arable Soil over a Decade, Regardless of Reduced Summer Precipitation. *Soil Biol. Biochem.* **2024**, *194*, 109439. [CrossRef]
37. Lak, Z.A.; Sandén, H.; Mayer, M.; Rewald, B. Specific Root Respiration of Three Plant Species as Influenced by Storage Time and Conditions. *Plant Soil* **2020**, *453*, 615–626. [CrossRef]
38. Wuest, S. Seasonal Variation in Soil Organic Carbon. *Soil Sci. Soc. Am. J.* **2014**, *78*, 1442–1447. [CrossRef]
39. Ekström, T. Leaching of Concrete: The Leaching Process and Its Effects. Ph.D. Thesis, Lund University, Lund, Sweden, 2003.
40. Bouzar, B.; Mamindy-Pajany, Y. Manufacture and Characterization of Carbonated Lightweight Aggregates from Waste Paper Fly Ash. *Powder Technol.* **2022**, *406*, 117583. [CrossRef]
41. Yu, D.; Duan, H.; Song, Q.; Li, X.; Zhang, H.; Zhang, H.; Liu, Y.; Shen, W.; Wang, J. Characterizing the Environmental Impact of Metals in Construction and Demolition Waste. *Environ. Sci. Pollut. Res.* **2018**, *25*, 13823–13832. [CrossRef]
42. Perry, P.M.; Pavlik, J.W.; Sheets, R.W.; Biagioni, R.N. Lead, Cadmium, and Zinc Concentrations in Plaster and Mortar from Structures in Jasper and Newton Counties, Missouri (Tri-State Mining District). *Sci. Total Environ.* **2005**, *336*, 275–281. [CrossRef] [PubMed]
43. Diotti, A.; Perèz Galvin, A.; Piccinali, A.; Plizzari, G.; Sorlini, S. Chemical and Leaching Behavior of Construction and Demolition Wastes and Recycled Aggregates. *Sustainability* **2020**, *12*, 10326. [CrossRef]
44. Madigan, M.T.; Bender, K.S.; Buckley, D.H.; Sattley, W.M.; Stahl, D.A. *Brock Biology of Microorganisms*, 16th ed.; Pearson: London, UK, 2020.
45. Philippot, L.; Chenu, C.; Kappler, A.; Rillig, M.C.; Fierer, N. The Interplay between Microbial Communities and Soil Properties. *Nat. Rev. Microbiol.* **2024**, *22*, 226–239. [CrossRef]
46. Bai, S.; Fan, M.; Wu, M.; Sui, X.; Song, Y.; Jiang, Y.; Meng, H.; Liu, Y.; Wang, X.; Hao, X.; et al. Crop Rotation and Organic Fertilizer Maintains Diversity and Activity of CbbL-Carrying CO_2-Fixing Bacteria in Reclaimed Coal Mining Soils. *Eur. J. Soil Biol.* **2025**, *126*, 103759. [CrossRef]
47. Zhang, Z.; Sun, J.; Wang, D.; Lin, T.; Yin, Y.; Wang, W.; Wang, Y.; Wang, Z.; Fan, L.; Jiao, X. Effects of Rotation Corn on Potato Yield, Quality, and Soil Microbial Communities. *Front. Microbiol.* **2025**, *16*, 1493333. [CrossRef]
48. DeBruyn, J.M.; Nixon, L.T.; Fawaz, M.N.; Johnson, A.M.; Radosevich, M. Global Biogeography and Quantitative Seasonal Dynamics of Gemmatimonadetes in Soil. *Appl. Environ. Microbiol.* **2011**, *77*, 6295–6300. [CrossRef]
49. Feng, Y.; Chen, H.; Fu, L.; Yin, M.; Wang, Z.; Li, Y.; Cao, W. Green Manuring Enhances Soil Multifunctionality in Tobacco Field in Southwest China. *Microorganisms* **2024**, *12*, 949. [CrossRef] [PubMed]
50. Jiang, Y.; Zhou, C.; Khan, A.; Zhang, X.; Mamtimin, T.; Fan, J.; Hou, X.; Liu, P.; Han, H.; Li, X. Environmental Risks of Mask Wastes Binding Pollutants: Phytotoxicity, Microbial Community, Nitrogen and Carbon Cycles. *J. Hazard Mater.* **2024**, *476*, 135058. [CrossRef] [PubMed]
51. Jia, R.; Qu, X.; Chen, M.; Xu, Y.; Liu, Z.; Peixoto, L.; Lin, Y.; Guo, Y.; Kumar, A.; Chen, J.; et al. Soil Microbial Variability in Contrasting Grown Flue-cured Tobacco under Long-term Continuous Cropping. *Soil. Use Manag.* **2025**, *41*, e70063. [CrossRef]
52. Mandic-Mulec, I.; Stefanic, P.; van Elsas, J.D. Ecology of *Bacillaceae*. *Microbiol. Spectr.* **2015**, *3*, 59–85. [CrossRef] [PubMed]
53. Zhu, K.; Jia, W.; Mei, Y.; Wu, S.; Huang, P. Shift from Flooding to Drying Enhances the Respiration of Soil Aggregates by Changing Microbial Community Composition and Keystone Taxa. *Front. Microbiol.* **2023**, *14*, 1167353. [CrossRef]
54. Kanjanasuntree, R.; Kim, J.-H.; Yoon, J.-H.; Sukhoom, A.; Kantachote, D.; Kim, W. *Arenimonas halophila* sp. nov., Isolated from Soil. *Int. J. Syst. Evol. Microbiol.* **2018**, *68*, 2188–2193. [CrossRef]
55. Xu, L.; Sun, J.-Q.; Liu, X.; Liu, X.-Z.; Qiao, M.-Q.; Wu, X.-L. *Arenimonas Soli* sp. Nov., Isolated from Saline–Alkaline Soil. *Int. J. Syst. Evol. Microbiol.* **2017**, *67*, 2829–2833. [CrossRef]

56. Zhao, J.; Wang, J.; Cui, B.; Zhai, B.; Hu, C.; Liu, Y.; Xia, L.; Liu, C.; Li, Z. Mixed Irrigation Affects the Composition and Diversity of the Soil Bacterial Community. *Open Geosci.* **2024**, *16*, 20220659. [CrossRef]
57. Gómez Expósito, R.; Postma, J.; Raaijmakers, J.M.; De Bruijn, I. Diversity and Activity of Lysobacter Species from Disease Suppressive Soils. *Front. Microbiol.* **2015**, *6*, 1243. [CrossRef] [PubMed]